Feasibility Study of a 10 MW MgB_2 Fully Superconducting Generator for Offshore Wind Turbines

Dimitris Kostopoulos, Dong Liu, Gaurav Genani, Henk Polinder
Delft University of Technology Mekelweg 4, 2628CD Delft, Netherlands
dimitkostopoulos@gmail.com, d.liu-1@tudelft.nl, gaurav.genani@gmail.com, h.polinder@tudelft.nl

Abstract

Offshore wind is considered a vital component of the future large scale renewable generation portfolio. Intense R&D effort is occurring in both the technology and the supply chain aiming at cost reduction.

The drivetrain of wind turbines is an area of continuous evolution with currently no one standard configuration in the industry. It is anticipated that in order to upscale offshore wind turbines in the 10+ MW power range innovation is necessary in this subsystem.

A possible solution could be the adoption of superconductivity technology. The potential benefits are multiple comprising weight, dimension and cost reduction in both capital and operating costs.

In this paper a rough analytical design is presented of an MgB_2 fully superconducting wind turbine generator (WTG). An analytical current sheet distribution is adopted to calculate the magnetic field of the generator and a finite element method (FEM) analysis is used to verify the field calculation. The objective of this work is to assess the technical feasibility of this generator topology and attempt to extract more general conclusions regarding the potential application of superconducting drivetrains in offshore wind turbines.

1. Why a superconducting WTG?

Increasing environmental awareness is progressively leading to a shift in electrical generation from fossil fuel power plants towards renewable solutions. Wind energy is a vital component of the renewable generation portfolio and is the renewable considered to be the most competitive with fossil fuels. Grid parity is still not a reality. However, the gap with conventional technology is closing in terms of levelized cost of energy (LCOE): from the 9.2 c€ /kWh for the 95 kW turbine of the '80s to 5.3 c€ /kWh for a 2,000 kW machine in 2006 [1], which is a remarkable improvement. Cost projections for the near future do not foresee a dramatic breakthrough in the reduction of the LCOE. However, there is a lot of potential in the mid and long term with estimates of grid parity for the best onshore sites already in 2015 and in 2023-25 for offshore wind [2].

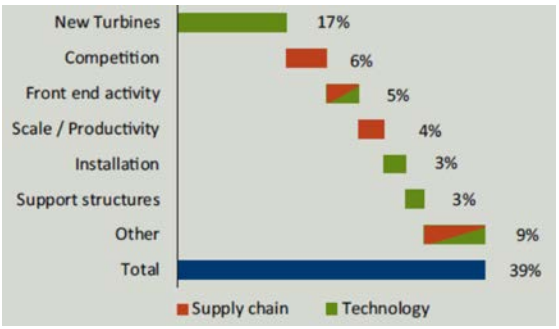


Figure 1 Offshore wind power cost reduction % potential in levelized cost of energy for projects with final investment decision in 2011 and in 2020 [4]

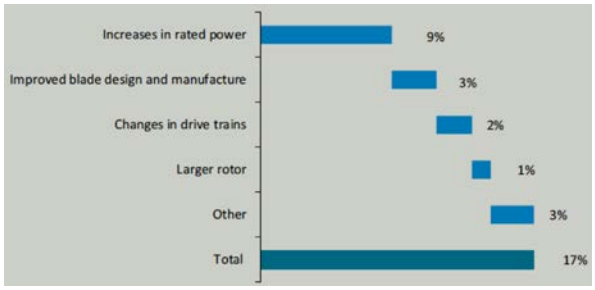


Figure 2 Offshore wind power cost reduction opportunities from changes in turbine technology [4]

Wind energy is a capital intensive business with many site specific cost factors. For onshore wind the turbine accounts in the total cost share to a range from 65% to 84%, whereas offshore from 30 to 50% [3, 4]. In offshore wind the presence of other important cost factors (foundations, grid connection, installation, maintenance etc.) diminishes the impact of the cost of the turbine itself to the overall cost and therefore wind turbine designs that could lead to a decrease of other

cost factors could still boost the feasibility of offshore wind farms

In this prospect in the offshore wind industry a trend is establishing itself consisting of a demand for larger turbines with a power rating in the 10+ MW range. The application of superconductivity in wind turbines could represent a valid and viable solution for this power range. In principle a superconducting electrical machine has a set of characteristics that lead to significant advantages. These include the already demonstrated advantages of [5]:

- Enhanced efficiency at all loads
- Higher power density
- Reduced weight and dimension

As well as the potential advantages of:

- Reduced acoustic noise
- Lower life cycle cost
- Reduced capital cost
- Enhanced grid stability
- Lower maintenance requirements

As an indication of the potential of superconducting technology some results of recent studies are given. An NREL study [6] has indicated that a partially high temperature superconducting (HTS) wind turbine generator design of American Superconductors could weigh 30% less than a permanent magnet (PM) generator (Fig. 1) with a 10% reduction of the capital cost.

In another study of innovation in wind turbines [7], the adoption of superconducting drive trains is indicated as potentially the second largest contributor in reducing LCOE. Apart the already mentioned mass and dimension reduction, a 2% reduction is anticipated in the overall turbine capital expenditure (CAPEX) and a 10% reduction in operating expenditure (OPEX) with an increased energy capture especially at partial loads.

Naturally, superconductivity is still not a mature technology. This is highlighted in both studies with long length wire availability, costs and technological risks as some of the major issues still to be addressed. Moreover, due to the relatively early stages of development there is no preferred layout and configuration of fully superconducting machines.

The exposed arguments give sufficient motivation to research this technology. In this paper is discussed the technical feasibility of the application of MgB_2 multi-pole direct drive fully superconducting wind turbine generators.

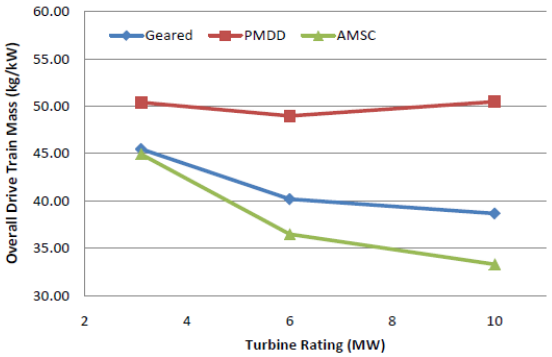


Figure 3 Comparison of overall drive train mass for geared, PMDD, and AMSC turbines [6]

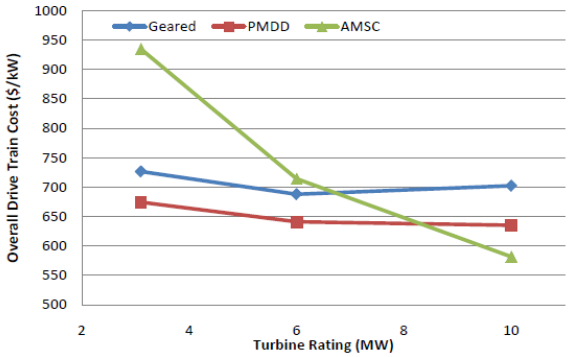


Figure 4 Comparison of overall drive train cost for geared, PMDD, and AMSC turbines [6]

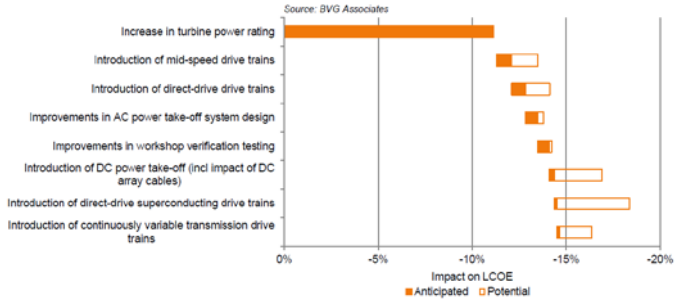


Figure 5 Anticipated and potential impact of turbine nacelle innovations [7]

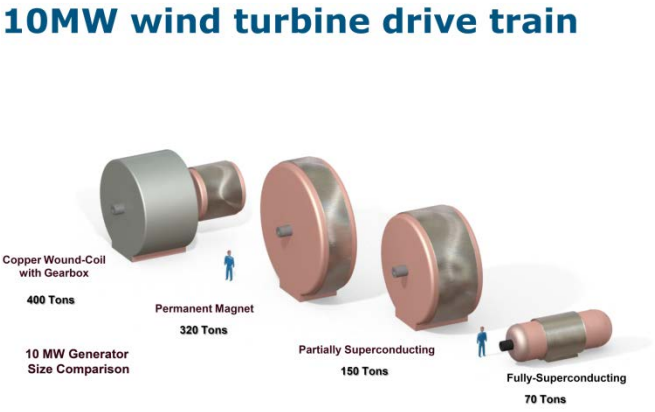


Figure 6 Comparison of 10 MW WTGs [8]

2. Methodology

In order to assess the generator's electromagnetic performance, an analytical approach is adopted based on equations found in the literature for the treatment of air-core machines [9]-[15].

The main concept in studying air-core machines consists of representing the effective winding distribution as a linear current distribution sine distributed over the periphery of the machine. . The HTS windings (both field and armature) are represented as rings contained between an outer and an inner radius as depicted in Fig. 7. The equivalent current sheets R_{fsheet} and R_{asheet} are taken to be the average of the outer and inner radii.

The assumptions of the electromagnetic model are the following:

- End effects neglected
- Eddy currents neglected
- Only the fundamental is considered
- Windings carry currents only in the z direction
- Windings approximated by sine distributed current sheets

The field calculation of the generator results by considering the ampere loading distribution over the periphery of the generator and successively evaluating its Fourier transformation.

$$K_r(\theta) = \sum K^{\nu}_{sheet} \sin(\nu p\theta) \ [\mathrm{A/m}] \qquad (1)$$

where K_r is the rotor current loading and p is the number of pole pairs. Harmonic analysis can be carried out by separating each component of the current sheet. In this study only the fundamental is considered. As a consequence:

$$K_r(\theta) = K_r \sin p\theta \ [A/m] \qquad (2)$$

The amplitude of the equivalent current sheet is defined as:

$$K_r = \frac{2N_r k_w}{\pi R_{fsheet}} * I_{sheet} \quad [\mathrm{A/m}] \qquad (3)$$

where I_{sheet} is the current of the HTS coils, N_r is the total number of turns of the rotor and k_w the winding factor.

In order to correctly define the equivalent rotor current sheet amplitude the positioning of the HTS coils should be considered. In Fig. 8 the position of the racetracks is indicated in the generator's cross section for a pole pair. The color depicts the direction of the current in the coils.

In a similar way the equivalent armature current sheet can be calculated. The only difference lies in the fact that there are three phases carrying currents displaced with respect to each other by 120°. The stator is divided into 2pm zones with the number of pole pairs *p* and the number of phases *m*. Each zone is carrying instantaneously current in the opposite direction as depicted in Fig. 9 with the different colors of the current carrying regions (3 phases 10 pole pairs). Each current zone represents a side of a racetrack.

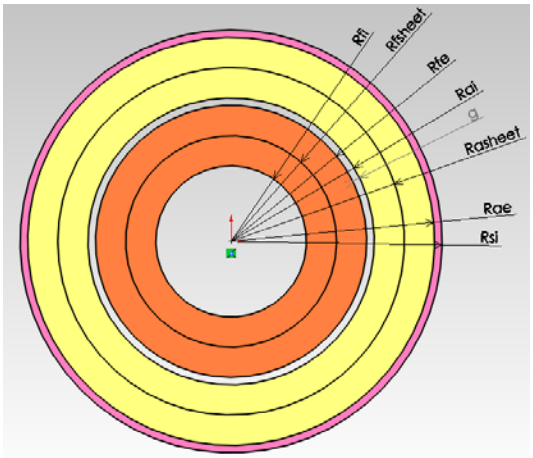


Figure 7 Cross section of the proposed generator

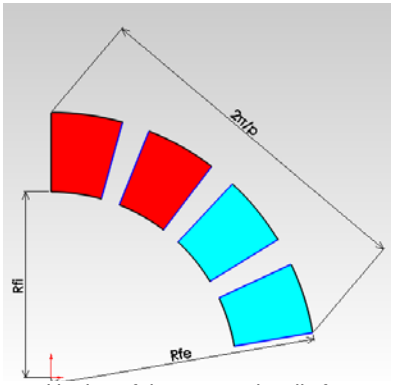


Figure 8 Positioning of the racetrack coils for a rotor pole pair

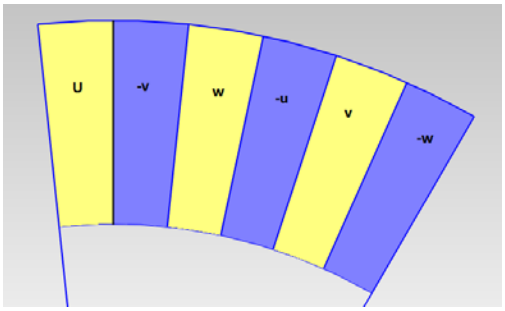


Figure 9 Stator pole pitch

The flux density of the generator is calculated by resolving the vector potential equation in the various regions (windings, shield and interfaces):

$$-\nabla^2 \vec{A} = \mu \vec{J} \quad (4)$$

where $\vec{A}$ is the magnetic vector potential and $\vec{J}$ is the electric current density. With the assumptions made the vector potential has a solution of the flowing type:

$$A = A_0(r) \sin p\theta \quad (5)$$

$A_0(r)$ is then the solution of the following equation (r generic radius):

$$\frac{d^2 A_0}{dr^2} + \frac{1}{r}\frac{dA_0}{dt} - \frac{p^2}{r^2} A_0 = 0 \quad (6)$$

Equation (6) can be solved with the following boundary conditions:

- $K = 0$ at $r = 0$ and $r = \infty$
- continuity of the radial component of the flux density B_r at the various region boundaries
- continuity of the tangential component of the magnetic intensity H_θ at the various region boundaries

The radial and tangential components of the flux density can then be calculated by:

$$B_r = \frac{1}{r}\frac{\partial A}{\partial \theta} \qquad \partial B_\theta = -\frac{\partial A}{\partial r} \quad (7)$$

The final expressions of the flux density have the form of the following equations valid outside the winding region. With r the generic radius the expressions of the field from the rotor current are:

For $r > R_{fsheet}$

$$Br = \frac{\mu_0 K_r}{2} \left(\frac{r}{R_r}\right)^{p+1} \cos p\theta \quad (8)$$

$$B_\theta = \frac{\mu_0 K_r}{2} \left(\frac{r}{R_r}\right)^{p+1} \sin p\theta \quad (9)$$

For $r < R_{fsheet}$

$$Br = \frac{\mu_0 K_r}{2} \left(\frac{r}{R_r}\right)^{p-1} \cdot \left[1 + \eta\lambda_s \left(\frac{R_r}{R_{s1}}\right)^{2p}\right] \cos p\theta \quad (10)$$

$$B_\theta = \frac{\mu_0 K_r}{2} \left(\frac{r}{R_r}\right)^{p-1} \left[1 + \eta\lambda_s \left(\frac{r}{R_{s1}}\right)^{2p}\right] (-\sin p\theta) \quad (11)$$

The expressions for the other regions are not given in this paper, but can be found in the literature [10]-[15],

For the verification of the field calculation a FEM analysis has been performed. A 2-D finite element model has been developed to take into account the actual field coil geometry. The materials and parameters are summarized in Table I. Magnetic saturation is taken into account in the environment shield iron. One pole (1/20th of the machine) is modeled, and the symmetry and periodical condition are used. The distance between the field coil and the armature coil is the effective air gap length which is 100 mm for this machine.

Material of field core	Air
Material of armature teeth	Air
Material of armature core	Air
Material of EM shield	Iron (with saturation)
Dimension of field coil	40 mm height, 149 mm width, 360 mm inner width
Mean radius of field coil	2.4 m
Dimension of armature coil	30 mm height, 180 mm width, 360 mm inner width
Mean radius of armature coil	2.5 m
Field current density	2.04×108 A/m2

Table 1 Materials and parameters used for FEM

3. Conceptual design of a 10 MW MgB_2 fully superconducting WTG

a. Introduction

The design of a fully superconducting machine differs in many aspects from the design of a conventional machine. Firstly, the possible omission of iron and consequently the large effective air gap means that the traditional computational methods are inadequate: the flux density cannot be assumed to cross the air gap perpendicularly and thus does not only consist of a radial component. The division between mutual and leakage flux is not as easily identifiable as in conventional machines where the main flux is the one that crosses the air gap, whereas the leakage flux consists of the one linking the iron teeth and of the end leakage. In air-core

machines there are no teeth and the field is two dimensional with the mentioned simplifying assumptions in section 2.

The adoption of the air-core topology also has consequences. The windings are experiencing torque and significant Lorentz forces due to the high field and high current densities. Superconducting machines have inherently low synchronous reactance. This fact on the one hand results in a stiff operational behaviour and on the other hand in fault situations the forces and currents are of larger magnitude which in turn increments the support structure requirements. In conventional machines iron also acts as a heat sink for the winding.

The fact that the machine operates at cryogenic temperatures sets limitations on the suitable materials. The construction materials should guarantee strength and endurance in thermal stresses and should provide support for the windings. At the same time the heat leakage through the materials should be minimized. The insulation should withstand the low operating temperature and the stress that arises from thermal contraction of different materials in the insulating wire. HTS wires are not typically sold as insulated products and depending on the technique used to produce the wire there are restrictions on the suitable materials.

As it emerges there are a large number of conflicting parameters to be taken into consideration and the detailed design of such a machine goes well beyond the scope of this paper. In the following subsections the objective is to provide an insight of the basic design options and present a rough conceptual design of a 10 MW HTS wind turbine generator.

b. Wire adopted

As already mentioned the HTS material used is magnesium diboride (MgB_2) due to the fact that currently seems the only viable HTS for AC use. In particular the reference products for this paper are the Hypertech wires, although there are also other wire producers (i.e. Columbus superconductors). Superconducting wires do not only contain superconductors and the addition of a matrix material is necessary for the stabilization of the superconductor. Usually copper is used. The exact amount of copper is a trade-off between stability, heat transfer, electromagnetic design and losses.

Compared to other materials, apart being superior in terms of AC losses MgB_2 also has large margin for improvement, lower cost and no issues regarding the maximum producible wire length. Table 2 summarizes the results.

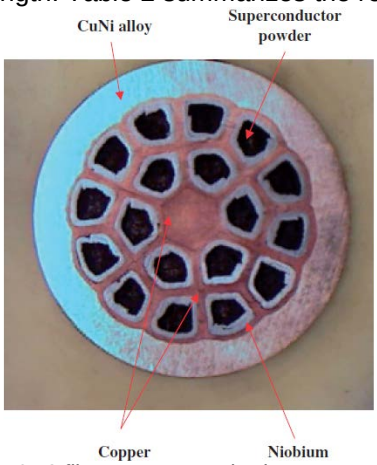


Figure 10 18 filament Hypertech wire cross section [95]

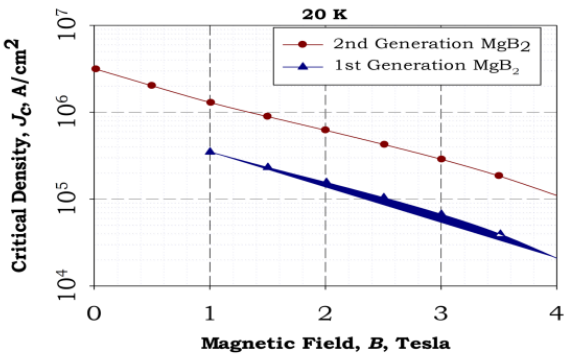


Figure 11 Hypertech MgB2 wire performance evolution [47]

LTS	HTS cuprates	MgB_2
Developed since the '60s	Developed since 1986	Developed since 2001
Very high performance	Good performance	Acceptable performance
Abrupt phase transition	Gradual phase transition	Gradual phase transition
Very low critical temperature	Higher critical temperature	Intermediate critical temperature
Round wires	Tapes	Tapes and round wires
High losses in AC use	High losses in AC use	Lower losses in AC use
Low stability	More stable	More stable

Table 2 MgB_2 comparison with other superconductors

c. Layout

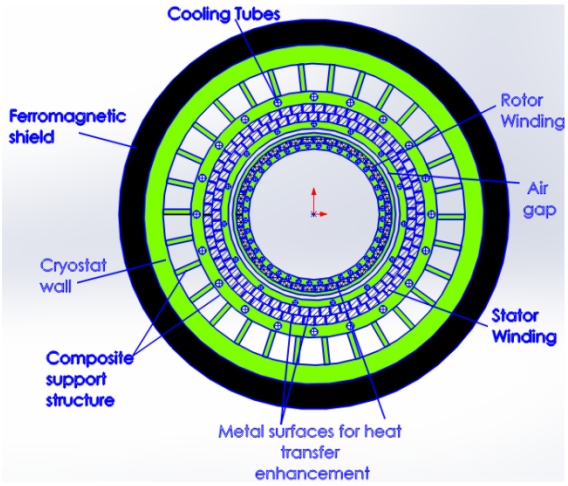


Figure 12 MgB_2 fully superconducting generator concept cross sectional view

The general outline of the generator is a fully superconducting machine with a non-magnetic rotor body housed in a single cryostat with an environmental shield that encloses the generator. Stator and rotor coils are both supported by a composite support structure. The major driver for the choice of composite material is weight.

As heat transfer mechanism the proposed design adopts the adiabatic forced flow winding concept [16]. The winding operates under high quality vacuum and is globally conduction cooled by the circulation of cryogen in pipes. The pipes are in contact with a metal surface that acts as a heat sink. In order to enhance the thermal conductivity within the winding the coils are impregnated with a substance (Stycast) making it almost a monolithic structure.

The environmental shield is included in the proposed design. It has the function to enclose the generator's field and generally to provide mechanical support to the cryostat. It can be ferromagnetic or conductive. In the first case it will be from laminated iron. The disadvantage is that it is heavy, although it attenuates well both AC and DC fields outside the machine, enhances the field in the machine and provides a stiff support structure. A conductive shield is a lighter option although it is not the preferable one. This is due to the incomplete attenuation provided (only AC fields) and to the fact that cannot be located in close proximity to the armature to avoid excessive losses and its demagnetizing effect [17].

d. Design options

The power rating is 10 MW. The phase RMS voltage is set to 10kV. As a consequence the steady state RMS rated phase current is approximately 340 A. It will be assumed that this current is applied from a full converter to the armature, as it is the usual scheme of connection of variable speed direct drive wind turbines.

The flux density level of the generator at the stator winding radius could be set at a much higher value respect to conventional machines. Fields of 3-4 T at 20 K are technically possible for recent 2nd generation MgB_2 wire. However, this is at the expense of a lower current density with subsequently more wire needed to produce a given magnetomotive force (mmf). With a more conservative approach the aimed peak flux density is set to 2 T at the stator winding radius. The corresponding field in the rotor winding area is not calculated due to the analytical electromagnetic model adopted. For the calculations are used the values of the critical current density corresponding to 3 T.

The operating temperature is fixed to 20 K in order to obtain satisfactory performance of the wires. The performance could be enhanced by lowering the temperature, but at the expense of higher costs for the cooling system and the use of less efficient devices that make the cooling system heavier and bulkier.

The number of pole pairs is set to be p=10. The motivation for this choice is that as reported in [14], this number of pole pairs decreases the harmonic content in the winding. Moreover, as reported in [18] a 20 pole machine is desirable because it yields a better efficiency and weight compared to machines with lower pole pairs and less wire consumption compared to machines with a higher number of pole pairs.

In many superconducting machines and electromagnetic shield (EM) is used to protect the rotor coils from AC fields and to damp the transient oscillations. The EM is made from a conductive material (copper or aluminum) and should be able to withstand the significant forces developed during faults. For this reason the conductive material layer is usually reinforced with a stainless steel or a composite support. Due to the material characteristics (low AC loss) and due to the overall topology (machine coupled with a full converter thus able to provide the damping

function) the EM shield is not included and the magnetic air gap is kept high.

Insulation at cryogenic temperatures is not a straight forward issue. LTS materials are typically sold as an insulated product, whereas for HTS there is no consolidated practice. Generally superconducting coils require turn to turn and layer to layer insulation. This means that the mechanical and the thermal properties of the composite structure of the insulated wire are highly anisotropic in all 3 directions [19]. Insulation is subjected to a number of different forces (shear, compression, tension and combinations of these) arising from both the magnetic and thermal loading. Thermal stresses arise as a result of the differences in expansion/contraction coefficients and local stresses arise at orthogonal interfaces even between materials with similar properties [19].

For the above mentioned arguments Kapton has been assumed as insulating materials because it:

- Is one of the few polymers to have a similar thermal coefficients as metals [20].
- Has excellent dielectric properties
- Has extraordinary high thermal conductivity for a polymer [21].
- Is supplied with an adhesive tape which ensures good contact with the conductor

On the downside of this insulating material is that it can “only” survive till 400°C thus making it inappropriate for “wind and react” wire. As a consequence the “react and wind” technique is adopted. The handling of this reacted wire requires extra care (i.e. in the process of winding the coil). MgB_2 wires are brittle and suffer severe degradation of their properties beyond a strain limit.

Operation at cryogenic temperatures has the consequence that radiative heat transfer plays an important role: since it scales with the 4^{th} power of the temperature difference, breaking out the process with the use of intermediate temperature thermal shields protects the coils more effectively. This can be done with the use of a metallic surface anchored at that intermediate temperature. Usually cryocoolers operating at 20 K have a 1st stage around 80 K. At this stage the losses through the structure and part of the current leads can be removed. Multi-layer insulation (MLI) is also deployed to lower radiation. The MLI usually consists of 0.5 μm thick aluminium coated Mylar or Kapton sheets in the vacuum space. The evacuation and the initial cool down are time consuming: there are gases absorbed from the surface of MLI blankets and the blankets require a lot of time to reach thermal equilibrium.

As already mentioned aiming at a low weight machine the material selection is restricted to composite materials. Composites have anisotropic properties depending on the direction of the beams and at the volumetric content of beams and matrix. Generally speaking comparing them to steel they can be 3 to 5 times stronger, 2 to 3 times stiffer and 3 to 4 times lighter [22].

The torque tube (TT) is a sensible part of a superconducting machine and there is very little detailed information available. The TT design should have the following characteristics [23]:

- Strong in torsion to transmit the torque
- Rigid to avoid vibrations
- Minimize the heat leakage
- Accommodate for the thermal deformation of the material

The first 2 properties are achieved through a large cross sectional moment of inertia and short length and are in conflict with the 3rd property that requires small cross sectional to length ratio. In many HTS prototypes composite torque tubes are used which achieve very small heat leakage and very robust behaviour. In [14] an investigation is carried out on the preferable shape of the TT comparing a hollow cylinder and a shaft. For the same torque capability the hollow cylinder is the one with lower heat leakage and this shape is assumed for the proposed generator. The rotor pole coils are mounted on the surface of the TT cylinder embedded in a “cage” type structure.

The stator support structure has to transmit the reaction torque to the wind turbine frame and at the same time support the coils in experiencing Lorentz forces. In order to fulfil the second function a “cage” type structure is assumed were the windings are embedded into composite slots. Cylinder geometry is assumed on the back of the stator winding supporting it and transmitting the reaction torque. The stator is successively mechanically connected to the cryostat walls through composite rods cantilevered to the cryostat wall.

e. Losses and thermal budget estimation

In order to estimate the thermal budget of the generator 2 items need to be considered, namely the internal loss of the machine and the following heat leakages:

- through the support structure
- through the TT

- from radiative heat transfer

On the contrary of a misleading common belief superconductors also exhibit losses. In addition to a small loss present in a DC operating condition there are AC dependant:

- Hysteresis loss
- Eddy current loss
- Self-field loss

There is an analogy between the magnetization of ferromagnetic materials and superconductors where also M-H loops are formed and therefore the loss can be computed from the area of the loop. AC losses in superconductors also suggest the fundamental difference that they have with normal conductors. Superconducting materials may be regarded as having their "skin effect" amplitude dependent whereas as it is known normal conductors have a frequency dependent skin effect.

The AC losses generally depend on:

- Operating temperature,
- Magnitude and direction of the magnetic field,
- Transport current
- Frequency
- Wire characteristics (filament diameter, twist pitch and matrix transverse resistivity)

For the calculation of the losses in superconductors numerical codes are required. With the analytical formulas used in this section only a rough estimation is possible. In principle there are 2 ways to calculate AC losses and this is or via the integration of in the wire volume or via the surface integral of the Poynting vector. Adopting the first approach this implies that knowledge about the magnetization of the superconductor is required. The calculation is conducted adopting the critical state model which assumes that the current density in the superconductor or is equal to the critical value or is zero. The common practice in AC loss calculation is to calculate singularly the various contribution and sum up for the total losses.

Important loss factors not considered in this paper affecting losses are:

- The magnetization of the material
- The current sharing between filaments

Other loss mechanisms not considered in this paper are:

- AC loss from wind load variations during steady state operation
- AC loss from initial ramp of coils to operating conditions
- AC loss from ripple currents during steady state operation

The DC loss of the field coils is calculated as follows. Defining $E(L)$ as the electric field in the superconductor as a function of length, I_T the coil transport current and I_C the coil critical current, the electromagnetic behaviour of superconductors is described by the power law [17]:

$$E(L) = E_0 \left(\frac{I_T}{I_C}\right)^n \qquad (12)$$

This relation reflects the industrial practice to consider the critical current of the superconductor as the current that produces a voltage drop of $E_0 = 1$ [μV/cm]. The value of the exponent n is an indication of how abrupt is the change from a superconducting to a resistive state and for Hypertech MgB_2 wires is around 15. A higher value means that the superconductor has lower DC losses. In order to calculate the DC loss of the field coils, first the voltage drop of the entire cable is calculated by integrating (12) over the length of the cable and consequently the power loss can be computed by multiplying the current of the wire with the corresponding voltage drop.

The formulas used to estimate the AC losses are based on [24]. For the hysteresis loss For the estimation of the AC losses the first step is to evaluate the penetration field B_p which is defined as (r_0: radius filament):

$$B_p = \frac{1}{\pi} 4 * \mu_0 * J_C * r_0 \text{ T} \qquad (13)$$

Defining $\mathcal{B}$ as:

$$\mathcal{B} = \frac{B_{max}}{B_p} \qquad (14)$$

where B_{max} is the amplitude of the applied field oscillation. The formula for the estimation of the hysteresis loss differs depending on whether the penetration field in higher the applied field which means evaluate if $\mathcal{B} > 1 \; or \; \mathcal{B} < 1$. Due to the loading conditions of the proposed design the following formula is used:

$$Q_h = \frac{B_{max}^2}{2\mu_0} * \left(\frac{4}{3\mathcal{B}} - \frac{0.71}{\mathcal{B}^2}\right) \text{ [J/cycle/m}^3\text{]} \qquad (15)$$

For the calculation of the eddy current losses the time constant of the wire is defined as:

$$\tau = \frac{\mu_0}{2\rho_e} * (\frac{l_p}{2\pi})^2 \quad (16)$$

where ρ_e is the wire matrix resistivity and l_p is the twist pitch of the wire. For the estimation of the coupling losses between filaments the following formula valid for sinusoidal field variation has been used:

$$Q_{cou} = \frac{B_{max}^2}{2\mu_0} * \frac{\pi\omega\tau}{(\omega\tau)^2 + 1} \ [\mathrm{J/cycle/m^3}\ ](17)$$

The last loss contribution that has been considered is the stator self-field loss due to the AC transport current. The following formula is used:

$$P_{self\ field} = \frac{1}{\pi} * \mu_0 * f * I_c^2 * f(i)\ \mathrm{W/m}\ (18)$$

With i defined as the ratio of the maximum value of the transport current to the critical coil current which results in the loss function:

$$f(i) = (1-i)\ln(1-i) + (2-i) * \frac{i}{2} \quad (19)$$

The Carnot efficiency of a cryocooler is defined as:

$$\eta_{carnot} = \frac{T_C}{T_W - T_C} \quad (20)$$

The coefficient of performance (COP) is the inverse of the efficiency and represents the ratio of power that should be given at room temperature to provide 1 W of cooling at cryogenic temperatures. For the operating temperature and assuming a cryocooler efficiency of 20% of Carnot (challenging objective to reach at 20 K with the current state of the art) we have a COP of around 93 and this value is used to estimate the required compressor power.

4. Results and conclusions

Tables 3 and 4 reassume the major properties of the proposed generator design that have been estimated through an analytical sinusoidal sheet distribution.

Generator type	Direct drive fully superconducting
Generator topology	Air-core with stator back iron
HTS material	MgB_2
Operating temperature	20 K
Support structure material	Composite G-10
Speed range	4-11 RPM
Rated power	10 MW
Number of poles	20
Phase voltage	10 kV
Rated RMS stator phase current	340 A
Field pole current	1350 A
Rotor electric loading	4.6 MA/m
Stator electric loading	174 kA/m
Total wire length estimation	55 km
Flux density at stator winding radius	2 T
Flux density at field winding radius	3 T
External diameter	5.6 m
Cryostat thickness	30 mm
Estimated weight	60-70 tons

Table 3 Design specifications

Rotor DC loss	100 W
Stator self field loss	10 W
Stator hysteresis loss	675 W
Stator filament coupling loss	380 W
Rotor hysteresis loss	2 W
Rotor filament coupling loss	1 W
Total internal loss	1.2 kW
Total external heat load	1 kW
Total heat budget @20 K	2.2 kW
Assumed COP	93
Required cooling power @300 K	205 kW
Other losses	2 %
Efficiency	97%

Table 4 Loss estimation

The FEM analysis has verified the field calculation of the fundamental of the flux density at the armature winding layer (B=2 T) and is depicted in Fig. 14. The magnetic field is only excited by the field current while the armature current is zero.

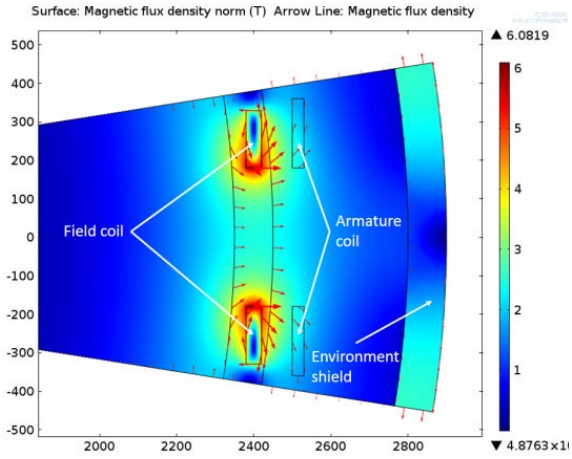


Figure 13 Flux density of one pole of the designed generator

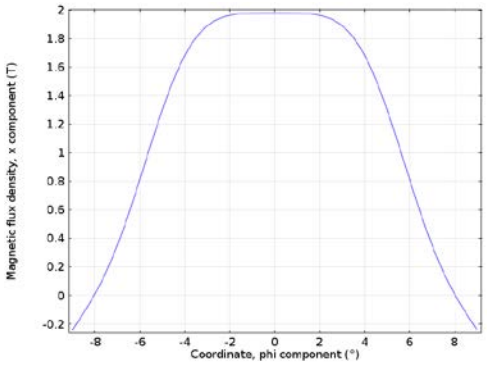


Figure 14 Flux density over one armature coil at the armature coil

It is noted in Fig. 13 that the maximum flux density occurring at the boundary of the field coil is approximately 6 T. The amplitude of the fundamental component in the field coil is about 3 T and fits the analytical calculation. However, FEM analysis was not conducted taking into account the material properties and therefore in reality boundary conditions are different.

The proposed generator design has good electrical performance and this would mean enhanced energy yield due to the flat efficiency curve of fully superconducting generators. However removing 2.2 kW at 20 K is still currently challenging. It can be concluded that :

- Fully superconducting multi-pole WTGs are not technically feasible due to cooling system requirements
- A low pole machine could be more feasible
- Partially superconducting generators are feasible with commercially available cryocoolers

5 References

[1] "The Economics of Wind Energy", A report by the European Wind Energy Association EWEA March 2009

[2] "EWEA – Energy Mix In Europe to 2050 Wind stands at the center of future energy generation" Make consultancy presentation in EWEA 2013 in Vienna, Austria

[3] "Renewable energy technologies: Cost analysis series, Volume 1: Power Sector Issue 5/5 Wind Power", IRENA working paper June 2012

[4] "Offshore Wind Cost Reduction Pathways Study" The crown estate May 2012

[5] J. F. Gieras, "Advancements in Electric Machines" Springer, 2010

[6] B. Maples, M. Hand, and W. Musial "Comparative Assessment of Direct Drive High Temperature Superconducting Generators in Multi-Megawatt Class Wind Turbines", NREL 2010

[7] "Offshore wind cost reduction pathways: Technology work stream" BVG associates May 2012

[8] History and Latest Development of Superconducting Machines B. B. Jensen, P. J. Masson ICEM 2012

[9] J. L. Kirtley , " Basic Formulas for Air Core Synchronous Machines , " Paper 71 CP 155 - PWR, Winter Power Meeting, IEEE, New York, 1971.

[10] T.J.E. Miller and A. Hughes: "Analysis of fields and inductances in air-cored and iron-cored synchronous machines", Proc. IEE, 1977,124, (2), pp. 121-126.

[11] T.H.E. Miller and A. Hughes: "Comparative design and performance analysis of air-cored and iron-cored synchronous machines" Proc. IEE, 124(2):127{132, 1977.

[12] Abrahamsen, A.B.; Mijatovic, N.; Seiler, E.; Sorensen, M.P.; Koch, M.; Norgard, P.B.; Pedersen, N.F.; Traeholt, C.; Andersen, N.H.; Ostergard, J.; , "Design Study of 10 kW Superconducting Generator for Wind Turbine Applications," Applied Superconductivity, IEEE Transactions on , vol.19, no.3, pp.1678-1682, June 2009

[13] N Mijatovic, A B Abrahamsen, C Træholt, E Seiler, M Henriksen1, V M Rodriguez-Zermeno and N F Pedersen "Superconducting generators for wind turbines: Design considerations" Journal of Physics Conference Series Volume 234 Part 3

[14] N Mijatovic "Superconducting Wind Turbine Generators" PhD thesis DTU 2012

[15] P. Tixador "Fully superconducting generators" Handbook of Applied Superconductivity, Volume 2 Edited by Bernd Seeber Taylor & Francis 1998 Pages 1553–1577

[16] Y. Iwasa "Case Studies in Superconducting Magnets: Design and Operational Issues" Springer 2009

[17] S.S. Kalsi, "Applications of high temperature superconductors to electric power equipment", John Wiley & Sons, April 2011

[18] N.Maki "Design study of high-temperature superconducting generators for wind power systems" IOP Science Journal of Physics: Conference Series 97 2008

[19] D Evans "Turn, layer and ground insulation for superconducting magnets", Physica C: Superconductivity, Volume 354, Issues 1–4, May 2001, Pages 136-142

[20] Jack W. Ekin "Experimental Techniques for Low-Temperature Measurements Cryostat Design, Material Properties, and Superconductor Critical-Current Testing" Oxford university press

[21] Kapton brochure downloaded from http://www2.dupont.com/Kapton/en_US/ last accessed in 28/11/2012
[22] V.S. GangaRao, P.V. Vijay, "Feasibility review of FRP materials for structural applications" West Virginia University 2010
[23] A. Bejan "Improved thermal design of the cryogenic cooling system for a superconducting synchronous generator PhD dissertation, Massachuetts Institute of Technology 1974
[24] Wilson "SUPERCONDUCTING MAGNETS" Oxford Science publications 1983